

Short Note

Petr Klímek, Václav Sebera*, Darius Tytko, Martin Brabec and Jaroslav Lukeš

Micromechanical properties of beech cell wall measured by micropillar compression test and nanoindentation mapping

<https://doi.org/10.1515/hf-2019-0128>

Received April 30, 2019; accepted November 22, 2019; previously published online xx

Abstract: Wood exhibits very different behavior and properties at different scales. One important scale is the cell wall (CW) that is commonly tested by nanoindentation. Common nanoindentation provides important insight into the material but has limitations because it does not apply uniaxial stress and provides data from single spots. Therefore, the aim was to examine beech CW using two state-of-the-art techniques: micropillar compression (MCo) and nanoindentation mapping (NIP). The mean strength of the beech CW was found to be about 276 MPa and the mean yield stress was 183 MPa. These values were higher than those in most cited literature, which was attributed to the fact that libriform fibers from beech late wood were measured. Mean E obtained from MCo was about 7.95 GPa, which was lower than the values obtained on a macrolevel and about 61% of the value obtained from NIP. NIP also showed that E of the CW around the middle lamella (ML) was about 64% of the value at the location attributed to the S_2 layer. Lower E from MCo may be caused by sinking of the micropillar into the wood structure under the load. Failure of the micropillars showed gradual collapse into themselves, with debonding at the S_3 layer or the MLs.

Keywords: beech, cell wall, mechanical properties, micropillar compression, nanoindentation

Introduction

Wood is a hierarchically organized material with many cellular and intercellular elements. These elements are, in general, co-responsible for mechanical behavior of wood. While structural mechanical properties, important for engineering, are tested, and testing is subjected to many standards, the micromechanical behavior is evaluated with various non-standardized techniques. A frequent technique for the evaluation of wood cell wall (CW) mechanical properties is the nanoindentation first introduced in wood science by Wimmer et al. (1997). This work was later followed by other investigations of different natural materials (Gindl and Gupta 2002; Gindl et al. 2004; Stoeckel et al. 2013; Arnould et al. 2017). Although nanoindentation was not found as a suitable method for determination of absolute values of wooden CW mechanical properties, it remains an appropriate method for comparative studies at the CW scale (Jäger et al. 2011). Aside from the fact that nanoindentation is not feasible for determination of absolute values of CW mechanical properties, there are other limitations for “stand-alone” nanoindentation such as lack of resolution when navigating across the sample and possibility to gain data from single spots only.

The first limitation – obtaining absolute mechanical properties – has been recently overcome by introducing focused ion beam (FIB) technology that enables creation of micro- to nano-samples that can be further tested in various ways. Orso et al. (2006) successfully used this approach to examine the modulus of elasticity (MOE) in bending of spruce CW and gained an MOE of about 28 GPa. The deflection was determined using a scanning electron microscope (SEM), and the force response was obtained by atomic force microscopy (AFM). More recently, effort was put on coupling FIB-SEM and nanoindentation for performing *in situ* compression tests of wood CW because they represent uniaxial loading cases. This approach was shown in Adusumalli et al. (2010) who analyzed spruce secondary CW in the longitudinal

*Corresponding author: Václav Sebera, InnoRenew CoE, Livade 6, 6310 Izola, Slovenia; Mendel University in Brno, Zemědělská 1, 61300 Brno, Czech Republic; and University of Primorska, 6000 Koper, Slovenia, e-mail: seberav@gmail.com

Petr Klímek: TESCAN a.s., Libušina tř. 1, 62300 Brno, Czech Republic

Darius Tytko: TESCAN GmbH, Zum Lonnenhohl 46, 44319 Dortmund, Germany

Martin Brabec: Mendel University in Brno, Zemědělská 1, 61300 Brno, Czech Republic

Jaroslav Lukeš: Bruker Nano Surfaces – Hysitron, Technická 4, Prague, Czech Republic

direction using the micropillar compression (MCo) test. Their results showed an average yield stress of about 160 MPa, biphasic stress-strain diagrams and strain hardening. Zhang et al. (2010) performed MCo on loblolly pine and Keranji and concluded that yield stress obtained by this approach does not depend on micropillar diameter. They further obtained an average yield stress and strength for loblolly pine of 111.3 MPa and 125 MPa, respectively, and for Keranji of 136.5 MPa and 160 MPa, respectively. In addition, they obtained nanoindentation modulus for loblolly pine in the range of 18.8 GPa and for Keranji of about 24.6 GPa. Raghavan et al. (2012) performed MCo on spruce samples created on an interface of two cells, i.e. containing middle lamella (ML), and compared them to samples containing only an S_2 layer. Samples with a ML experienced lower strength than pure S_2 layer samples, but the failure occurred at the interface of the S_1 and S_2 layers, not at the interface with the ML. A similar approach of creating microsamples, using femtosecond laser machining (FLM), was recently presented in Jakob et al. (2017). The authors created both compression and dog-bone-shaped tension microsamples that were tested under a stereomicroscope. They found lower values for the tensile strength than the measured yield strength from nanoindentation and pillar compression tests obtained elsewhere in the literature. A possible explanation for such differences lies in a size effect – nanoindentation provides data from smaller areas compared to MCo. A combination of MCo and continuum micromechanical modeling to obtain phase properties of inhomogeneous materials was presented by Schwiedrzik et al. (2016). The authors showed that the S_2 layer of the Norway spruce CW exhibited a median yield stress of 146.5 MPa for normal wood and 45.3 MPa for compression wood. Their prediction showed a very good accuracy by taking into

account the orientation of microfibrils in the CW layers. More recently, Qin et al. (2018) utilized nanoindentation mapping (NIP) for examining larch sapwood CWs and showed that this technique can be used to reveal subtle variations in micromechanical properties of individual layers of the wood CW.

Testing at the micro- to nano-levels is becoming important because it may obtain more precise absolute values for material properties of wood. One of the new techniques that widens the possibility of exploration at these levels is E mapping that obtains full-field data of E and hardness without the necessity of making a classical imprint, as is the case for traditional single-spot nanoindentation. Therefore, the goal of this study was to (1) provide new data of beech average CW elasticity as well as data along its thickness and (2) compare the MCo test with data obtained by E mapping using NIP.

Materials and methods

Micropillar preparation and testing: Due to the fact that MCo was carried out in a different device other than elastic modulus mapping, we created twin specimens that were taken from one larger specimen of approximately $10 \times 10 \times 5 \text{ mm}^3$. This ensured that measurements were made on wood of the same origin with very similar characteristics. Micropillars were prepared from a CW of beech wood (*Fagus sylvatica* L.). A cube of beech wood with dimensions of $5 \times 5 \times 5 \text{ mm}^3$ was placed on an aluminum stub with a diameter of 12 mm and inserted into the chamber of a SEM equipped with a Ga^+ FIB column, named TESCAN S8000G (TESCAN ORSAY HOLDING a.s., Brno, Czech Republic). As soon as vacuum was ready, six micropillars with an average diameter of $4 \mu\text{m}$ and $10 \mu\text{m}$ in length were prepared from the wood CWs of libriform fibers located in late wood (Figure 1). The dimensions of the micropillar were chosen to have an aspect ratio (length/diameter) below 5 following the recommendations in Zhang et al. (2006).

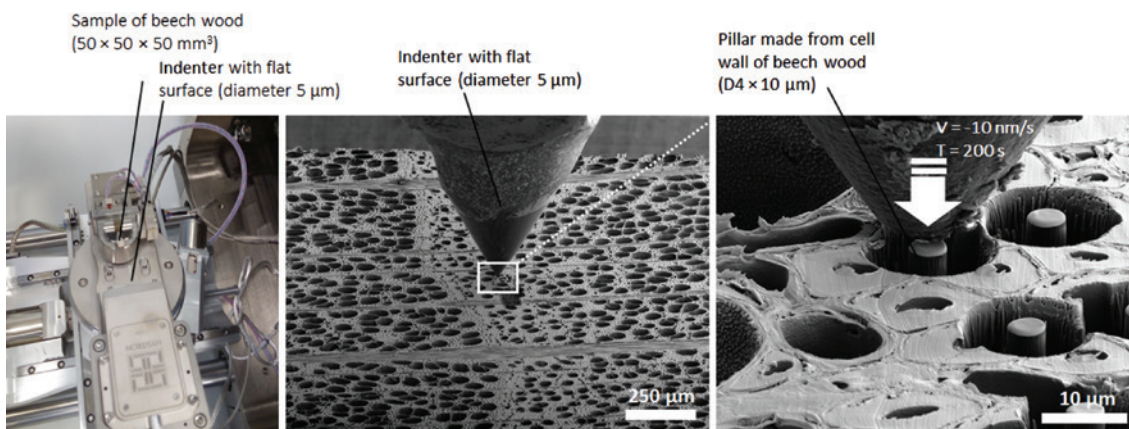


Figure 1: Micropillar compression at various scales.

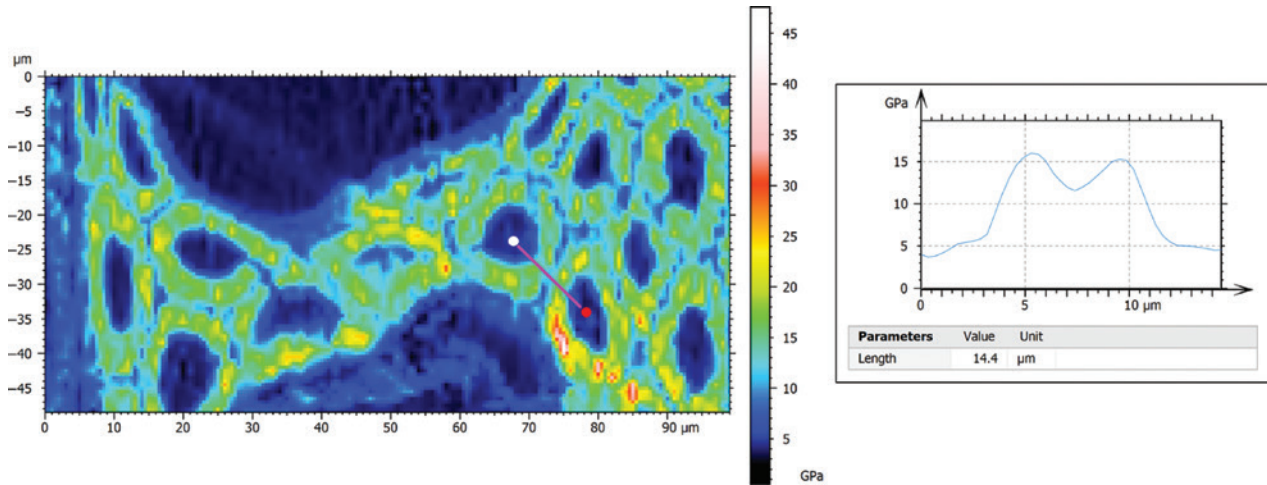


Figure 2: Resulting color-scale mapping of the E and an E -profile across two CWs. High-speed indentation data of sample no. 2 showing E -modulus map (left image) and E -modulus profile (right image). The profile (profile no. 6) corresponds to the line shown in the map.

First, a platinum deposition was made at five regions of interest (ROIs) using an opti-gas injection system and FIB at 30 keV voltage and 150 pA current. Subsequently, rounded trenches were milled around the depositions with the FIB operating at 30 keV and 5 nA current. The pillars were polished to the final diameter by clockwise circular polishing (as defined in TESCAN Drawbeam) at a voltage of 30 keV and a current of 100 pA. The pillars were visualized and measured on the SEM micrographs before and after testing. *In situ* tests on the pillars were conducted in the chamber of the FIB-SEM using a Hysitron PI 88 SEM picoIndenter (Bruker, Billerica, MA, USA) equipped with a flat punch indenter having a diameter of 5 μm . The indenter was navigated above the surface of the pillars *in situ* inside the SEM chamber. While observing and recording the testing process by SEM, all pillars were tested in compression. The loading rate of the picoIndenter was 10 nm s^{-1} and each pillar was tested until failure (end time 200 s). Displacement and force values were recorded and resulted in stress-strain curves. The elastic moduli were calculated from a linear part of the stress-strain curves defined by stresses at 78 MPa and 158 MPa. The yield stress was derived using a graphical technique (in ImageJ software) from the point where the tangent distorted at an angle of 3° with respect to the linear part of the stress-strain curve. To find out to what extent the micropillar sinks into the wood structure due to compression, simplified finite element analyses for various lengths of wood base were carried out (see Supplementary Table S1 for material properties, boundary conditions and geometrical model).

Elastic modulus mapping: The E was further examined using high-speed mechanical property mapping using the iMicro nanoindentation system from Nanomechanics, Inc. (Oak Ridge, TN, USA) in conjunction with the NanoBlitz3D method (Roa et al. 2018). In this testing procedure, an indentation test takes less than a second. This opens the possibility to test areas with a large number of indents in a reasonable time. Resulting data give the lateral distribution of the mechanical properties (e.g. gradients, trends) and can be evaluated statistically. To measure samples with this technique, the wood lumens had to be filled by an epoxy resin in order to stabilize the CW and yield a continuous flat surface. The indentation consisting of multiple sample analysis was carried out using a Berkovich

indenter and an applied force of 0.2 mN. Regions of $120 \times 50 \mu\text{m}$ were tested using a lateral resolution of 1 μm that represents the distance between the indents. This yielded a total number of 6000 indents. Figure 2 shows the resulting color-scale mapping of the E (Figure 2, left image) and an E -profile across two CWs (Figure 2, right image), which corresponds to the line marked in the map (Figure 2, left image). As the profile contains semi-continuous information with a step equal to $\sim 0.4 \mu\text{m}$ from two adjacent CWs, one can directly compare the absolute values of both CWs and evaluate the transition of E . In total, two samples were examined using the elastic modulus (E) mapping technique, where six profiles were analyzed from each sample, yielding 12 CWs per sample.

Results and discussion

The beech wood samples were first tested by MCo, and their stress-strain diagrams are shown in Figure 3, left image. The stress was calculated assuming a constant cross-section of the micropillar (engineering stress). The strain was calculated assuming the original length of the micropillar to be 10 μm . As seen from Figure 3, the stress-strain curves of the micropillars exhibited a biphasic course that is in agreement with Adusumalli et al. (2010). After reaching the first peak of maximal stress, the curves (except one) possessed a certain plateau with slow decrease. Then the stress started to slowly increase again, indicating stress hardening. For this reason, the strength was calculated at the first peak before the plateau region occurred.

The E mapping was conducted on two specimens. At each specimen, six profiles containing two adjacent CWs were created (Figure 3, right image). Because the profile shows discrete values that are not comparable to micropillar specimens in size, ROI was defined based on the

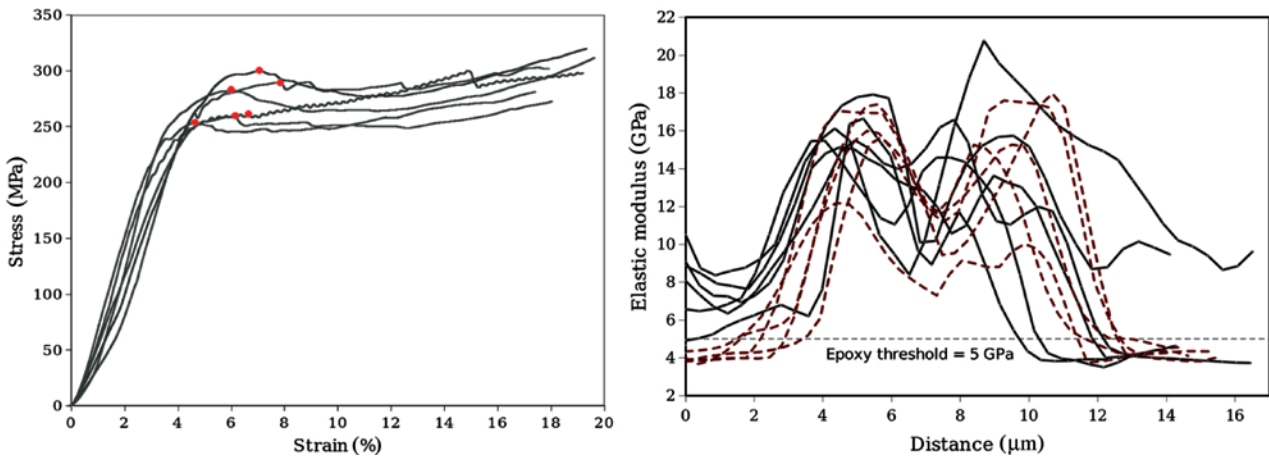


Figure 3: The stress-strain curves of the micropillars exhibited a biphasic course. Stress-strain diagrams from the MCo, with highlighted strengths (left image); Elastic moduli profiles for both specimens obtained by NIP, distinguished by different types of lines (right image).

values around the peaks in each profile with a width of $4\ \mu\text{m}$, which was the diameter of the pillars used for the compression tests. By this approach, the obtained E was more comparable to the one obtained from the MCo tests. The reason for it is probably more representative amount of CW material tested, which is also present in the volume of the micropillars. For instance, the ROI contains all the CW layers as tested during MCo. The right image in Figure 3 shows that each profile has two peaks that correspond to the positions with the assumedly highest proportion of S_2 layer at both CWs. The use of nanoindentation ROI in a size of a micropillar diameter gives an average value of E across the CW thickness similarly as in the case of MCo. However, because both techniques apply different boundary conditions and different material organization

at a given volume, their mutual comparison in terms of E is limited. The valley between both peaks in the profiles corresponds to a position of the CW with the highest proportion of a ML. The elastic modulus obtained by NIP may be slightly influenced by the resin that filled lumens or penetrated the CW material.

A summary of the results obtained by both techniques used to analyze the beech CW is listed in Table 1, showing data obtained by MCo and E mapping. Because the latter produced more data, the following needs to be clarified: “Cell wall profile mean E ” represents the mean value for each of the two peaks (according to both adjacent CWs) analyzed by the profile at ROI. The cell wall minimum (CW min) represents the mean E value of the valley between both peaks and may be attributed to the ML.

Table 1: Results from micropillar compression and elastic modulus mapping.

		1	2	3	4	5	6	Mean	CoV (%)	Std. dev.	
Micropillar testing	σ_y (MPa)	174	185	204	172	187	179	183	6.47	11.9	
	σ (MPa)	270	283	290	300	253	259	276	6.59	18.2	
	E (GPa)	8.22	9.06	8.61	7.25	8.16	6.42	7.95	12.1	0.96	
E mapping (Gpa)	Spec. no.1	Cell wall profile mean E (GPa)	13.6	13.6	15.2	13.06	14.0	11.5			
			13.1	12.0	13.7	16.9	10.4	9.91	13.1	14.9	1.94
		1 st CW max (GPa)	15.5	15.1	17.9	16.1	16.6	16.7			
		2 nd CW max (GPa)	14.6	13.6	15.7	20.8	12.0	11.7	15.6	17.4	2.72
		CW min (GPa)	11.1	10.6	10.1	8.39	11.1	8.93	9.81	11.4	1.12
	Spec. no. 2	Cell wall profile mean E (GPa)	14.6	14.4	10.2	12.2	17.8	13.5			
			13.0	15.5	8.67	13.4	11.4	12.8	13.1	18.3	2.41
		1 st CW max (GPa)	17.4	17.1	12.2	15.6	19.5	16.0			
			2 nd CW max (GPa)	15.3	17.6	10.0	18.0	13.4	15.3	15.5	18.6
		CW min (GPa)	11.7	11.2	7.30	9.45	11.0	11.6	10.1	17.4	1.76

σ_y , Yield stress; σ , strength; E , elastic modulus; CW, cell wall; CoV, coefficient of variation; Std. dev., standard deviation. 1st CW max and 2nd CW max are maximal values obtained from result profiles from NIP.

As seen from Table 1, the average yield stress provided by MCo (183 ± 11.9 MPa) was higher than the values in the cited literature. For instance, Raghavan et al. (2012) obtained a yield strength of about 125 ± 20 MPa and Adusumalli et al. (2010) obtained 158 ± 20 MPa from five micropillars, both investigated for spruce latewood. The obtained higher strength and yield stress can be attributed to the fact that a species different from that in mentioned literature was measured and, moreover, to the fact that libriform fibers in late wood zone were measured. Such fibers have a pure mechanical function in beech wood and their microfibril angle (MFA) is about 0° across the whole diameter of the trunk (Lichtenegger et al. 1999). The numerical model predicting yield stress depending on MFA introduced by Schwiedrzik et al. (2016) would prescribe the yield stress to be higher than 200 MPa for a CW with such a low MFA, the value of which is close to the range of our data.

On average, the E obtained from the MCo tests was 7.95 GPa, which was lower than the values obtained by nanoindentation techniques in the literature. The mean E from the MCo tests was 61% of E obtained from the E mapping (as averaged on the ROI of the E profiles). The lower E obtained from the MCo can be primarily attributed to the fact that the micropillar itself is not laid on a stiff pad, but on the wood structure. Therefore, the micropillars are pressed into the wood structure by the applied force that, consequently, results in lower obtained stiffness. The impact of such micropillar “sinking” can be substantial and up to approximately 40% as shown by simplified finite element analyses (see Supplementary Table S1 and Supplementary Figures S1 and S2). The rotation of the micropillars was not observed at the SEM images (see Supplementary Figure S3). The lower value of E obtained by MCo tests may be attributed to the fact that a micropillar represents a situation that the CW was not naturally designed for – isolated CW material without any connection to a network of cells. Lastly, the size and shape of the micropillar may also be causing lower E due to the hierarchical structure of the wood CW. Visual analysis of a failure revealed that all micropillars collapsed into themselves by a gradual compression. The failure occurred either at the S_3 layer or in the ML (see Supplementary Figure S3). This represents a different failure mechanism from the one observed in Raghavan et al. (2012) that consisted of a tearing of the interface between the S_1 and the S_2 layers of the CW.

NIP showed that on average, the E at the position most likely possessing a ML was between 63% and 65% of the maximal E value in the profiles, i.e. at the position attributed to the most likely location of the S_2 layer. The E

obtained from the profile does not necessarily correspond to the E of the particular CW layer because the measurement of each point could be influenced by its surrounding, similarly as in standard hardness tests. However, the average E of the assumable S_2 layer was 1.5 times higher than for a position where ML was most likely to occur. This was a lower difference than was obtained by Qin et al. (2018) who showed 2 times higher values for the S_2 with respect to the ML.

Conclusions

1. The mean strength (σ), mean yield stress (σ_y) and mean elastic modulus (E) of beech CWs of libriform fibers in latewood provided by MCo were about 276 MPa, 175 MPa and 7.95 GPa, respectively.
2. The mean value of E obtained by the MCo was approximately 1.5 times lower than the mean values obtained by NIP and was most likely due to a “sinking” of the micropillars into the wood structure below. This should be of concern whenever MCo without an extraction of micropillars on a stiff pad is to be carried out.
3. Mean σ and mean σ_y obtained by MCo were higher than those in cited literature and may be attributed to the following: (i) the examined hardwood species as in all cited literature only softwood species are studied, and (ii) that the measured libriform fibers of beech late wood possess very low MFA that assumedly results in high mean values of σ and σ_y .
4. Failure of the micropillars occurred at their edges, which represented either the surface inside the lumen (S_3 layer) or the ML in between the CWs. The failure could be described as a gradual collapse of micropillars into themselves.

Author contributions: All the authors have accepted responsibility for the entire content of this submitted manuscript and approved submission.

Research funding: Horizon 2020 Framework Programme of the European Union; H2020 WIDESPREAD-2-Teaming: #739574, and the Republic of Slovenia, Investment funding of the Republic of Slovenia and the European Union of the European Regional Development Fund, as well as Slovenian Research Agency for funding infrastructural program, IO-0035.

Employment or leadership: None declared.

Honorarium: None declared.

References

- Adusumalli, R.B., Raghavan, R., Ghisleni, R., Zimmermann, T., Michler, J. (2010) Deformation and failure mechanism of secondary cell wall in Spruce late wood. *Appl. Phys. A* 100:447–452.
- Arnould, O., Siniscalco, D., Bourmaud, A., Le Duigou, A., Baley, C. (2017) Better insight into the nano-mechanical properties of flax fibre cell walls. *Ind. Crop. Prod.* 97:224–228.
- Gindl, W., Gupta, H.S. (2002) Cell-wall hardness and Young's modulus of melamine-modified spruce wood by nano-indentation. *Compos. A: Appl. Sci. Manuf.* 33:1141–1145.
- Gindl, W., Gupta, H.S., Schöberl, T., Lichtenegger, H.C., Fratzl, P. (2004) Mechanical properties of spruce wood cell walls by nanoindentation. *Appl. Phys. A: Mater. Sci. Process.* 79:2069–2073.
- Jäger, A., Hofstetter, K., Buksnowitz, C., Gindl-Altmutter, W., Konnerth, J. (2011) Identification of stiffness tensor components of wood cell walls by means of nanoindentation. *Compos. A: Appl. Sci. Manuf.* 42:2101–2109.
- Jakob, S., Pfeifenberger, M.J., Hohenwarter, A., Pippan, R. (2017) Femtosecond laser machining for characterization of local mechanical properties of biomaterials: a case study on wood. *Sci. Technol. Adv. Mater.* 18:574–583.
- Lichtenegger, H., Reiterer, A., Stanzl-Tschegg, S.E., Fratzl, P. (1999) Variation of cellulose microfibril angles in softwoods and hardwoods –possible strategy of mechanical optimization. *J. Struct. Biol.* 128:257–269.
- Orso, S., Wegst, U.G.K., Arzt, E. (2006) The elastic modulus of spruce wood cell wall material measured by an in situ bending technique. *J. Mater. Sci.* 41:5122–5126.
- Qin, L.Z., Lin, L.Y., Fu, F., Fan, M.Z. (2018) Micromechanical properties of wood cell wall and interface compound middle lamella using quasistatic nanoindentation and dynamic modulus mapping. *J. Mater. Sci.* (2018) 53:549–558.
- Raghavan, R., Adusumalli, R.B., Buerki, G., Hansen, S., Zimmermann, T., Michler, J. (2012) Deformation of the compound middle lamella in spruce latewood by micro-pillar compression of double cell walls. *J. Mater. Sci.* 47:6125–6130.
- Roa, J.J., Sudharshan Phani, P., Oliver, W.C., Llanes, L. (2018) Mapping of mechanical properties at microstructural length scale in WC-Co cemented carbides: assessment of hardness and elastic modulus by means of high speed massive nanoindentation and statistical analysis. *Int. J. Refract. Met. Hard Mater.* 75:211–217.
- Schwiedrzik, J., Raghavana, R., Rüggeberg, M., Hansen, S., Wehrs, J., Adusumalli, R.B., Zimmermann, T., Michler, J. (2016) Identification of polymer matrix yield stress in the wood cell wall based on micropillar compression and micromechanical modelling. *Philos. Mag.* 96:3461–3478.
- Stoeckel, F., Konnerth, J., Gindl-Altmutter, W. (2013) Mechanical properties of adhesives for bonding wood – a review. *Int. J. Adhes. Adhes.* 45:32–41.
- Wimmer, R., Lucas, B.N., Oliver, W.C., Tsui, T.Y. (1997) Longitudinal hardness and Young's modulus of spruce tracheid secondary walls using nanoindentation technique. *Wood Sci. Technol.* 31:131–141.
- Zhang, H., Schuster, B.E., Wei, Q., Ramesh, K.T. (2006) The design of accurate micro-compression experiments. *Scr. Mater.* 54:181–186.
- Zhang, X., Zhao, Q., Wang, S., Trejo, R., Lara-Curzio, E., Du, G. (2010) Characterizing strength and fracture of wood cell wall through uniaxial micro-compression test. *Compos. A: Appl. Sci. Manuf.* 41:632–638.

Supplementary Material: The online version of this article offers supplementary material (<https://doi.org/10.1515/hf-2019-0128>).